Journal of chemical & engineering data

Article

pubs.acs.org/jced

Solid–Liquid Equilibria of the Na_2SO_4 + $H_2NCH_2CH_2SO_3H$ + H_2O System from (288.15 to 328.15) K

Jie Lu,*[,†] Xun Zhou,[†] Lian-Wei Chen,[†] Li-Juan Zhang,[‡] and Sohrab Rohani[§]

[†]School of Chemical and Material Engineering, Jiangnan University, Wuxi 214122, China

[‡]School of Chemistry and Chemical Engineering, Shanghai University of Engineering Science, Shanghai 201620, China

[§]Department of Chemical and Biochemical Engineering, The University of Western Ontario, London, Ontario N6A 5B9, Canada

ABSTRACT: Solid–liquid equilibrium (SLE) and solution density data for the (Na_2SO_4 + $H_2NCH_2CH_2SO_3H$ + H_2O) system from (288.15 to 328.15) K were measured by use of the method of isothermal dissolution. From the experimental data, a set of polynomial equations were derived to calculate the solubility of taurine as a function of sodium sulfate mass fraction in the equilibrium solution, and two phase diagrams at (293.15 and 318.15) K were constructed. In general, the density of the equilibrium solution regularly increases with the sodium sulfate concentration. Furthermore, at low temperatures the equilibrium solid phase is $Na_2SO_4 \cdot 10H_2O$, whereas at high temperatures the equilibrium solid phase is Na_2SO_4. All of these data will provide a better understanding of the separation of taurine from Na_2SO_4 aqueous solutions through crystallization.

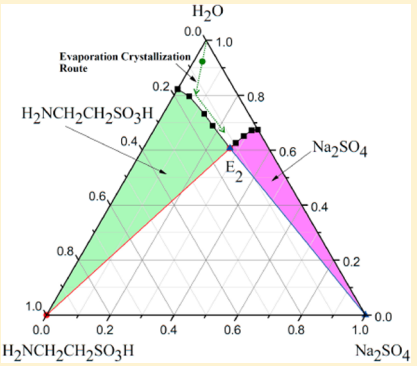

INTRODUCTION

Taurine ($H_2NCH_2CH_2SO_3H$), which is widely distributed in such organs as the heart, brain, and liver has been demonstrated to participate in physiological processes such as detoxification, antioxidation, osmoregulation, membrane stabilization, immunity, and so on.[1−5] To date, the hypocholesteolemic effect of taurine in mice and humans has been established.[6−8] Therefore, taurine is usually encouraged to act as a food additive.[9−11]

In current industrial production, synthetic taurine is mainly obtained by the following two-step process:[12]

$$H_2NCH_2CH_2OH + SO_3 \rightarrow H_2NCH_2CH_2OSO_3H$$

$$H_2NCH_2CH_2OSO_3H + Na_2SO_3 \rightarrow H_2NCH_2CH_2SO_3H + Na_2SO_4$$

In the resulting mixture, sodium sulfate exists as a byproduct that must be removed to obtain pure taurine.

Crystallization from solution is generally a common unit operation for separating chemical species and producing solids with specific properties as well. Effective design and scale-up of crystallization requires an understanding of solid–liquid phase behavior. Accurate phase diagrams can dictate the mode of operation and can define the operational window to avoid excessive nucleation and the formation of undesired solid forms. Therefore, the investigation of the thermodynamic phase equilibria (i.e., the characterization of phase diagrams) is of theoretical and practical importance. To date, a number of works have been conducted to describe the thermodynamic phase equilibria of the systems Na_2SO_4 + X + H_2O, where X = Li_2SO_4, $Na_2B_4O_7$, NaOH, Na_2MoO_4, $NaBrO_3$, and so on.[13−17] However, no study of the solid–liquid phase equilibria of the system Na_2SO_4 + $H_2NCH_2CH_2SO_3H$ + H_2O has been reported to date. Accordingly, the present work will contribute this system's solid–liquid equilibrium (SLE) and density data from (288.15 to 328.15) K, which were obtained by the use of the method of isothermal dissolution.

EXPERIMENTAL SECTION

Materials and Apparatus. Sodium sulfate (anhydrous, 0.995 in mass fraction) and taurine (0.990 in mass fraction) were purchased from Sinopharm Chemical Reagent Company (Shanghai, China) and used as received without further purification. Deionized water at pH 6.6 for the preparation of the solutions was produced in-house with a conductivity of $<1 \cdot 10^{-5}$ $S \cdot m^{-1}$. A THZ-82A thermostatic water bath shaker (Ronghua Instrument Manufacture Co., Ltd., Jintan, China) was employed for the solid–liquid mixing at each desired temperature with a precision of 0.1 °C. The densities (ρ) of equilibrium solutions were determined by the use of a DMA 4500 M digital densimeter with a precision of $1.0 \cdot 10^{-5}$ $g \cdot cm^{-3}$ (Anton Paar, Austria). The equilibrium solid phase was identified using a D8 ADVANCE powder X-ray diffractometer (Bruker AXS, Karlsruhe, Germany).

Experimental Procedure. In this work, the method of isothermal dissolution was employed.[18,19] In brief, a series of mixtures of sodium sulfate, taurine, and water with different compositions were loaded into various cleaned conical flasks and capped tightly with rubber caps, and then the flasks were put into the water bath shaker of which the temperature was

Received: April 10, 2014
Accepted: May 5, 2014
Published: May 12, 2014

   dx.doi.org/10.1021/je5003303 | J. Chem. Eng. Data 2014, 59, 2115−2119

controlled at the required value, rotating at 135 rpm to accelerate the solid−liquid equilibrium. Every half hour, a small volume of liquid from each of those flasks in which solid still existed was removed for analyses of composition and content. The observation that the composition and content of the liquid became constant indicated that SLE had been achieved. Then the shaker was stopped for 2 h to allow the solid to settle out of the liquid. At last, the supernatants were filtered, and their composition, content, and density were analyzed, whereas the solid phase was checked by X-ray diffraction. All of the experimental content and density data reported are averages of at least three repetitive measurements with a relative standard deviation 3.0 %.

The content of taurine in each solution was measured by a formaldehyde method using phenolphthalein as an indicator.[20] The sulfate ion concentration (SO_4^{2-}) was determined gravimetrically using barium chloride as a precipitant.[21]

RESULTS AND DISCUSSION

Tables 1 to 9 list the SLE data for the Na_2SO_4 + $H_2NCH_2CH_2SO_3H$ + H_2O system from (288.15 to 328.15) K. Meanwhile, the densities of equilibrium solutions at (293.15 and 313.15) K are shown in Tables 2 and 6.

Table 1. Experimental SLE Data for the System Na_2SO_4 (1) + $H_2NCH_2CH_2SO_3H$ (2) + H_2O (3) as Mass Fractions w at Temperature T = 288.15 K and Pressure p = 0.1 MPa[a]

no.	w_1	w_2	w_3	equilibrium solid phase
1	0	0.0766	0.9234	$H_2NCH_2CH_2SO_3H$
2	0.0216	0.0721	0.9063	$H_2NCH_2CH_2SO_3H$
3	0.0514	0.0681	0.8805	$H_2NCH_2CH_2SO_3H$
4	0.0741	0.0636	0.8623	$H_2NCH_2CH_2SO_3H$
5	0.0847	0.0567	0.8586	$H_2NCH_2CH_2SO_3H$ + $Na_2SO_4{\cdot}10H_2O$
6	0.0914	0.0469	0.8617	$Na_2SO_4{\cdot}10H_2O$
7	0.0963	0.0378	0.8659	$Na_2SO_4{\cdot}10H_2O$
8	0.1123	0.0092	0.8785	$Na_2SO_4{\cdot}10H_2O$
9	0.1187	0	0.8813	$Na_2SO_4{\cdot}10H_2O$

[a]Standard uncertainties (u) are $u(p)$ = 0.005 MPa, $u(T)$ = 0.1 K, and $u(w)$ = 0.0005.

Table 2. Experimental SLE Data for the System Na_2SO_4 (1) + $H_2NCH_2CH_2SO_3H$ (2) + H_2O (3) as Mass Fractions w and Densities ρ at Temperature T = 293.15 K and Pressure p = 0.1 MPa[a]

no.	w_1	w_2	w_3	ρ/g·cm^{-3}	equilibrium solid phase
D_1	0	0.0901	0.9099	1.0362	$H_2NCH_2CH_2SO_3H$
2	0.0282	0.0873	0.8845	1.0758	$H_2NCH_2CH_2SO_3H$
3	0.0740	0.0809	0.8451	1.1165	$H_2NCH_2CH_2SO_3H$
4	0.1153	0.0773	0.8074	1.1740	$H_2NCH_2CH_2SO_3H$
E_1	0.1413	0.0647	0.794	1.2374	$H_2NCH_2CH_2SO_3H$ + $Na_2SO_4{\cdot}10H_2O$
6	0.1487	0.0538	0.7975	1.2290	$Na_2SO_4{\cdot}10H_2O$
7	0.1669	0.0243	0.8088	1.2167	$Na_2SO_4{\cdot}10H_2O$
8	0.1731	0.0154	0.8115	1.2041	$Na_2SO_4{\cdot}10H_2O$
C_1	0.1812	0	0.8188	1.2027	$Na_2SO_4{\cdot}10H_2O$

[a]Standard uncertainties (u) are $u(p)$ = 0.005 MPa, $u(T)$ = 0.1 K, and $u(w)$ = 0.0005.

On the basis of the SLE data listed in Tables 1 and 7, two phase diagrams at (293.15 and 318.15) K, respectively, were schematically drawn, as shown in Figures 1 and 2. It is obvious

Table 3. Experimental SLE Data for the System Na_2SO_4 (1) + $H_2NCH_2CH_2SO_3H$ (2) + H_2O (3) as Mass Fractions w at Temperature T = 298.15 K and Pressure p = 0.1 MPa[a]

no.	w_1	w_2	w_3	equilibrium solid phase
1	0	0.1052	0.8969	$H_2NCH_2CH_2SO_3H$
2	0.0335	0.0983	0.8678	$H_2NCH_2CH_2SO_3H$
3	0.0797	0.0908	0.8282	$H_2NCH_2CH_2SO_3H$
4	0.1317	0.0871	0.7790	$H_2NCH_2CH_2SO_3H$ + $Na_2SO_4{\cdot}10H_2O$
5	0.1815	0.0771	0.7414	$Na_2SO_4{\cdot}10H_2O$
6	0.1997	0.0528	0.7481	$Na_2SO_4{\cdot}10H_2O$
7	0.2134	0.0282	0.7584	$Na_2SO_4{\cdot}10H_2O$
8	0.2185	0.0203	0.7612	$Na_2SO_4{\cdot}10H_2O$
9	0.2221	0	0.7779	$Na_2SO_4{\cdot}10H_2O$

[a]Standard uncertainties (u) are $u(p)$ = 0.005 MPa, $u(T)$ = 0.1 K, and $u(w)$ = 0.0005.

Table 4. Experimental SLE Data for the System Na_2SO_4 (1) + $H_2NCH_2CH_2SO_3H$ (2) + H_2O (3) as Mass Fractions w at Temperature T = 303.15 K and Pressure p = 0.1 MPa[a]

no.	w_1	w_2	w_3	equilibrium solid phase
1	0	0.1228	0.8772	$H_2NCH_2CH_2SO_3H$
2	0.0205	0.1143	0.8652	$H_2NCH_2CH_2SO_3H$
3	0.0972	0.1031	0.7997	$H_2NCH_2CH_2SO_3H$
4	0.1709	0.0960	0.7331	$H_2NCH_2CH_2SO_3H$ + $Na_2SO_4{\cdot}10H_2O$
5	0.2401	0.0858	0.6741	$Na_2SO_4{\cdot}10H_2O$
6	0.2612	0.0603	0.6785	$Na_2SO_4{\cdot}10H_2O$
7	0.2726	0.0406	0.6858	$Na_2SO_4{\cdot}10H_2O$
8	0.2887	0.0171	0.6942	$Na_2SO_4{\cdot}10H_2O$
9	0.2924	0	0.7076	$Na_2SO_4{\cdot}10H_2O$

[a]Standard uncertainties (u) are $u(p)$ = 0.005 MPa, $u(T)$ = 0.1 K, and $u(w)$ = 0.0005.

Table 5. Experimental SLE Data for the System Na_2SO_4 (1) + $H_2NCH_2CH_2SO_3H$ (2) + H_2O (3) as Mass Fractions w at Temperature T = 308.15 K and Pressure p = 0.1 MPa[a]

no.	w_1	w_2	w_3	equilibrium solid phase
1	0	0.1317	0.8683	$H_2NCH_2CH_2SO_3H$
2	0.0306	0.1267	0.8427	$H_2NCH_2CH_2SO_3H$
3	0.1049	0.1166	0.7785	$H_2NCH_2CH_2SO_3H$
4	0.1467	0.1092	0.7441	$H_2NCH_2CH_2SO_3H$
5	0.2579	0.0924	0.6497	$H_2NCH_2CH_2SO_3H$ + Na_2SO_4
6	0.2725	0.0735	0.6540	Na_2SO_4
7	0.2950	0.0408	0.6642	Na_2SO_4
8	0.3174	0.0132	0.6694	Na_2SO_4
9	0.3279	0	0.6721	Na_2SO_4

[a]Standard uncertainties (u) are $u(p)$ = 0.005 MPa, $u(T)$ = 0.1 K, and $u(w)$ = 0.0005.

that the phase diagrams at (288.15, 298.15, and 303.15) K shall be similar to that in Figure 1, while those at (308.15, 313.15, 323.15, and 328.15) K shall be similar to that in Figure 2.

In the phase diagrams shown in Figures 1 and 2, A_1 (A_2) and F_1 (F_2) represent pure solid $H_2NCH_2CH_2SO_3H$ and Na_2SO_4, respectively; D_1 (D_2) represents the solubility of $H_2NCH_2CH_2SO_3H$ in pure water at 293.15 K (318.15 K); C_1 (C_2) represents the solubility of Na_2SO_4 in pure water at 293.15 K (318.15 K); and B1 represents the solubility of $Na_2SO_4{\cdot}10H_2O$ in pure water at 293.15 K. D_1E_1 and D_2E_2 are boundary curves along which the saturated solutions are in equilibrium with solid $H_2NCH_2CH_2SO_3H$, while C_1E_1 and C_2E_2 are boundary curves along which the saturated solutions

dx.doi.org/10.1021/je5003303 | J. Chem. Eng. Data 2014, 59, 2115−2119

Table 6. Experimental SLE Data for the System Na_2SO_4 (1) + $H_2NCH_2CH_2SO_3H$ (2) + H_2O (3) as Mass Fractions w and Densities ρ at Temperature T = 313.15 K and Pressure p = 0.1 MPa[a]

no.	w_1	w_2	w_3	ρ/g·cm^{-3}	equilibrium solid phase
1	0	0.1476	0.8524	1.0584	$H_2NCH_2CH_2SO_3H$
2	0.0217	0.1417	0.8366	1.0922	$H_2NCH_2CH_2SO_3H$
3	0.0704	0.1352	0.7944	1.1624	$H_2NCH_2CH_2SO_3H$
4	0.1830	0.1279	0.6891	1.2280	$H_2NCH_2CH_2SO_3H$
5	0.2755	0.1061	0.6184	1.3348	$H_2NCH_2CH_2SO_3H$ + Na_2SO_4
6	0.2870	0.0886	0.6244	1.3316	Na_2SO_4
7	0.3067	0.0555	0.6378	1.3298	Na_2SO_4
8	0.3245	0.0262	0.6493	1.3247	Na_2SO_4
9	0.3312	0	0.6688	1.3244	Na_2SO_4

[a]Standard uncertainties (u) are $u(p)$ = 0.005 MPa, $u(T)$ = 0.1 K, and $u(w)$ = 0.0005.

Table 7. Experimental SLE Data for the System Na_2SO_4 (1) + $H_2NCH_2CH_2SO_3H$ (2) + H_2O (3) as Mass Fractions w at Temperature T = 318.15 K and Pressure p = 0.1 MPa[a]

no.	w_1	w_2	w_3	equilibrium solid phase
D_2	0	0.1782	0.8218	$H_2NCH_2CH_2SO_3H$
2	0.0495	0.1545	0.7960	$H_2NCH_2CH_2SO_3H$
3	0.1280	0.1397	0.7323	$H_2NCH_2CH_2SO_3H$
4	0.1758	0.1352	0.6890	$H_2NCH_2CH_2SO_3H$
E_2	0.2716	0.1212	0.6072	$H_2NCH_2CH_2SO_3H$ + Na_2SO_4
6	0.2802	0.0935	0.6263	Na_2SO_4
7	0.2926	0.0559	0.6515	Na_2SO_4
8	0.3072	0.0207	0.6721	Na_2SO_4
C_2	0.3256	0	0.6744	Na_2SO_4

[a]Standard uncertainties (u) are $u(p)$ = 0.005 MPa, $u(T)$ = 0.1 K, and $u(w)$ = 0.0005.

Table 8. Experimental SLE Data for the System Na_2SO_4 (1) + $H_2NCH_2CH_2SO_3H$ (2) + H_2O (3) as Mass Fractions w at Temperature T = 323.15 K and Pressure p = 0.1 MPa[a]

no.	w_1	w_2	w_3	equilibrium solid phase
1	0	0.1905	0.8095	$H_2NCH_2CH_2SO_3H$
2	0.0421	0.1862	0.7717	$H_2NCH_2CH_2SO_3H$
3	0.1181	0.1769	0.7330	$H_2NCH_2CH_2SO_3H$
4	0.1813	0.1687	0.6406	$H_2NCH_2CH_2SO_3H$
5	0.2601	0.1418	0.5981	$H_2NCH_2CH_2SO_3H$ + Na_2SO_4
6	0.2758	0.1025	0.6217	Na_2SO_4
7	0.2869	0.0703	0.6428	Na_2SO_4
8	0.3031	0.0329	0.6640	Na_2SO_4
9	0.3218	0	0.6782	Na_2SO_4

[a]Standard uncertainties (u) are $u(p)$ = 0.005 MPa, $u(T)$ = 0.1 K, and $u(w)$ = 0.0005.

are in equilibrium with solid $Na_2SO_4·10H_2O$ and Na_2SO_4, respectively. Point E_1 is the invariant point of the Na_2SO_4 + $H_2NCH_2CH_2SO_3H$ + H_2O at system 293.15 K, at which the equilibrium solid contains both $H_2NCH_2CH_2SO_3H$ and $Na_2SO_4·10H_2O$. Point E_2 is the invariant point at 318.15 K, at which the equilibrium solid contains both $H_2NCH_2CH_2SO_3H$ and Na_2SO_4. $W_1C_1D_1$ and $W_2C_2D_2$ are unsaturated regions at (293.15 and 318.15) K, respectively; $D_1E_1A_1$ and $D_2E_2A_2$ are crystalline regions of pure $H_2NCH_2CH_2SO_3H$ at (293.15 and 318.15) K, respectively; $C_1E_1B_1$ is the crystalline region of pure $Na_2SO_4·10H_2O$ at

Table 9. Experimental SLE Data for the System Na_2SO_4 (1) + $H_2NCH_2CH_2SO_3H$ (2) + H_2O (3) as Mass Fractions w at Temperature T = 328.15 K and Pressure p = 0.1 MPa[a]

no.	w_1	w_2	w_3	equilibrium solid phase
1	0	0.2028	0.7972	$H_2NCH_2CH_2SO_3H$
2	0.0510	0.1939	0.7551	$H_2NCH_2CH_2SO_3H$
3	0.1152	0.1879	0.6969	$H_2NCH_2CH_2SO_3H$
4	0.2006	0.1791	0.6203	$H_2NCH_2CH_2SO_3H$
5	0.2561	0.1527	0.5912	$H_2NCH_2CH_2SO_3H$ + Na_2SO_4
6	0.2661	0.1335	0.6004	Na_2SO_4
7	0.2922	0.0766	0.6312	Na_2SO_4
8	0.3127	0.0333	0.6540	Na_2SO_4
9	0.3161	0	0.6839	Na_2SO_4

[a]Standard uncertainties (u) are $u(p)$ = 0.005 MPa, $u(T)$ = 0.1 K, and $u(w)$ = 0.0005.

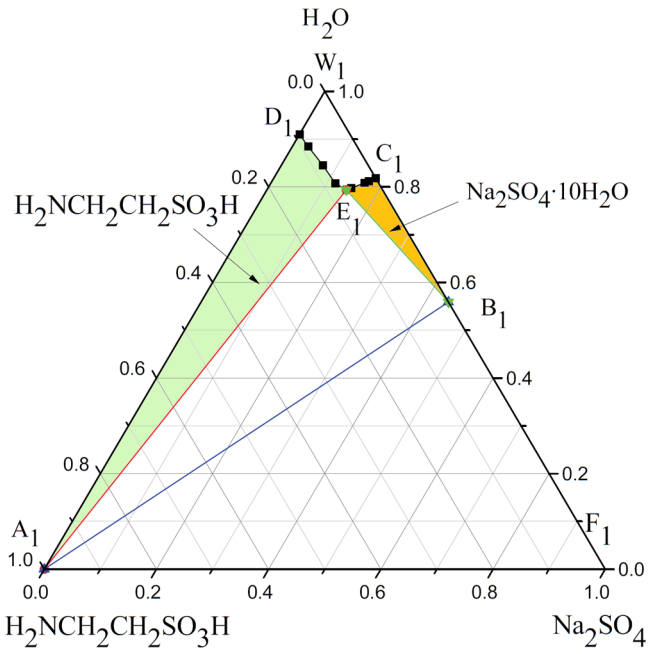

Figure 1. SLE phase diagram of Na_2SO_4 + $H_2NCH_2CH_2SO_3H$ + H_2O at T = 293.15 K (■, experimental points).

293.15 K, whereas $C_2E_2F_2$ is that of pure Na_2SO_4 at 318.15 K. In particular, in Figure 1, $A_1B_1E_1$ is the crystallization area of $H_2NCH_2CH_2SO_3H$ and $Na_2SO_4·10H_2O$, and $A_1B_1F_1$ is the crystallization area of $H_2NCH_2CH_2SO_3H$, $Na_2SO_4·10H_2O$, and Na_2SO_4, while in Figure 2, $A_2E_2F_2$ is the crystalline region of the mixture of $H_2NCH_2CH_2SO_3H$ and Na_2SO_4.

From above the tables and figures it can be seen that temperature can influence this solid−liquid equilibrium system. When the temperature is increased from (293.15 to 318.15) K, the unsaturated region apparently becomes larger, and $Na_2SO_4·10H_2O$ is transformed into Na_2SO_4 at high temperatures. In addition, the crystalline region of $H_2NCH_2CH_2SO_3H$ is larger than that of pure $Na_2SO_4·10H_2O$ or Na_2SO_4 because that the solubility of sodium sulfate is greater than that of taurine at a given temperature.

Following the works of Carton et al.,[22] Hu et al.,[23] and Ostroff and Metler,[24] the following expression was also employed to simulate the mass fractions of taurine in the equilibrium solutions:

$$\ln Y = A + Bw_1 + Cw_1^2 + Dw_1^3 + Ew_1^4 + Fw_1^5 \quad (1)$$

dx.doi.org/10.1021/je5003303 | J. Chem. Eng. Data 2014, 59, 2115−2119

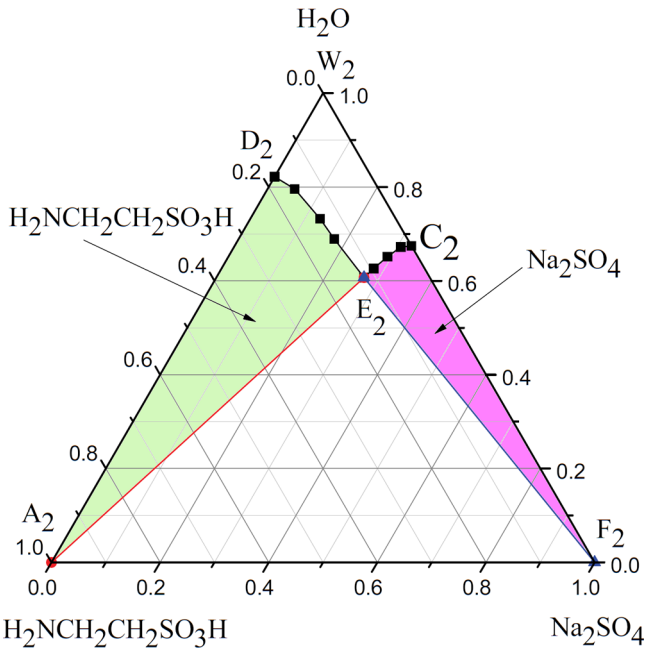

Figure 2. SLE phase diagram of Na_2SO_4 + $H_2NCH_2CH_2SO_3H$ + H_2O at T = 318.15 K (■, experimental points).

where Y and w_1 denote the mass fractions of taurine and sodium sulfate in the equilibrium solutions, respectively. The parameters A, B, C, D, E, and F as well as the corresponding standard deviations (σ) are given in Table 10. The calculated standard deviations show that eq 1 can be generally employed to simulate the solubility of taurine in aqueous solutions of sodium sulfate satisfactorily.

CONCLUSIONS

Phase equilibria for the Na_2SO_4 + $H_2NCH_2CH_2SO_3H$ + H_2O ternary system between (288.15 and 328.15) K have been investigated by use of the method of isothermal dissolution. The experimental results show that the system does not form solid solutions or complex salts. When the temperature is increased from (288.15 to 328.15) K, the unsaturated region becomes larger and the $Na_2SO_4{\cdot}10H_2O$ solid phase is transformed into Na_2SO_4. This work shall provide a fundamental basis for the separation of taurine from aqueous solutions of sodium sulfate by evaporation or cooling crystallization.

AUTHOR INFORMATION

Corresponding Author

*E-mail: Dr.LuJie@gmail.com. Fax: +86 510 85917763.

Funding

This work was financed by grants from the National Natural Science Foundation of China (21176102 and 21176215), the Natural Science Foundation of Jiangsu Province (BK20131100), and the Sino-German Center for Research Promotion (GZ935).

Notes

The authors declare no competing financial interest.

REFERENCES

(1) Wright, C. E.; Tallan, H. H.; Lin, Y. Y. Taurine: Biological update. *Annu. Rev. Biochem.* **1986**, *55*, 427−453.

(2) Chesney, R. W. Taurine: Its biological role and clinical implications. *Adv. Pediatr.* **1985**, *32*, 1−42.

(3) Huxtable, R. J. Physiological actions of taurine. *Physiol. Rev.* **1992**, *72*, 101−163.

(4) Birdsall, T. C. Therapeutic applications of taurine. *Altern. Med. Rev.* **1998**, *3*, 128−136.

(5) Saransaari, P.; Oja, S. S. Taurine and neural cell damage. *Amino Acids* **2000**, *19*, 509−526.

(6) Nakamura-Yamanaka, Y.; Tsuji, K.; Ichikawa, T. Effect of dietary taurine on cholesterol 7a-hydroxylase activity in the liver of mice fed a lithogenic diet. *J. Nutr. Sci. Vitaminol.* **1987**, *33*, 239−243.

(7) Murakami, S.; Kondo-Ohta, Y.; Tomisawa, K. Improvement in cholesterol metabolism in mice given chronic treatment of taurine and fed a high-fat diet. *Life Sci.* **1998**, *64*, 83−91.

(8) Mizushima, S.; Nara, Y.; Sawamura, M.; Yamori, Y. Effects of oral taurine supplementation on lipids and sympathetic nerve tone. *Adv. Exp. Med. Biol.* **1996**, *403*, 615−622.

(9) Heird, W. C. Taurine in neonatal nutrition—Revisited. *Arch. Dis. Child* **2004**, *89*, F473−F474.

(10) Zhang, M.; Izumi, I.; Kagamimori, S.; Sokejima, S.; Yamagami, T.; Liu, Z.; Qi, B. Role of taurine supplementation to prevent exercise-induced oxidative stress in healthy young men. *Amino Acids* **2004**, *26*, 203−207.

(11) Baum, M.; Weiss, M. The influence of a taurine containing drink on cardiac parameters before and after exercise measured by echocardiography. *Amino Acids* **2001**, *20*, 75−82.

(12) Marvel, C. S.; Bailey, C. F.; Sarberg, M. S. Synthesis of taurine. *J. Am. Chem. Soc.* **1927**, *49*, 1833−1837.

(13) Guo, Y. F.; Liu, Y. H.; Wang, Q. Phase equilibria and phase diagrams for the aqueous ternary system (Na_2SO_4 + Li_2SO_4 + H_2O) at (288 and 308) K. *J. Chem. Eng. Data* **2013**, *58*, 2763−2767.

(14) Cui, R. Z.; Sang, S. H.; Zhang, K. J. Phase equilibria in the ternary systems K_2SO_4−$K_2B_4O_7$−H_2O and Na_2SO_4−$Na_2B_4O_7$−H_2O at 348 K. *J. Chem. Eng. Data* **2012**, *57*, 3498−3501.

Table 10. Values of the Parameters in Equation 1

T/K	A	B	C	D	E	F	σ^a
288.15	−2.5692	−5.4273	265.10	−9446.9	150745	−865014	0.0057
293.15	−2.4070	−3.2387	164.18	−4161.5	40593	−135051	0.0083
298.15	−2.2516	−5.7271	201.28	−3506.4	24818	−60222	0.0044
303.15	−2.0955	−6.4096	170.03	−2164.7	11294	−20274	0.0093
308.15	−2.0272	−2.7705	76.832	−1074.4	5726.7	−10221	0.0074
313.15	−1.9114	−3.3186	71.060	−856.77	4344.4	−7511.1	0.0081
318.15	−1.7249	−11.371	304.30	−3397.8	15700	−25109	0.0051
323.15	−1.6586	−3.5233	129.49	−1704.0	8644.2	−14984	0.0094
328.15	−1.5714	−4.6316	115.41	−1275.6	5973.0	−9959.4	0.0075

$^a\sigma = \{\sum[(Y^{calc} - Y^{exp})^2/N]\}^{0.5}$, where Y^{calc} is the value calculated using eq 1, Y^{exp} is the experimental datum, and N is the total number of experimental data at the given temperature.

(15) Ding, A. J.; Wang, Y. J.; Ma, S. H. Phase diagram for the Na_2SO_4–NaOH–H_2O system and Na_2SO_4 solubility in sodium aluminate solution with caustic ratios of 12 and 15 at 80 °C. *J. Chem. Eng. Data* **2013**, *58*, 964–968.
(16) Ricci, J. E. The ternary system Na_2SO_4–$NaBrO_3$–H_2O, and a sixth possible type of solid solution formation between two components in the Roozeboom classification. *J. Am. Chem. Soc.* **1935**, *57*, 805–810.
(17) Ricci, J. E.; Linke, W. F. The quaternary system $MgMoO_4$–Na_2SO_4–H_2O at 25 °C and its related ternary systems. *J. Am. Chem. Soc.* **1951**, *73*, 3607–3612.
(18) Deng, T. L.; Yin, H. A.; Tang, M. L. Experimental and predictive phase equilibrium of the Li^+, Na^+/Cl^-, CO_3^{2-}–H_2O system at 298.15 K. *J. Chem. Eng. Data* **2002**, *47*, 26–29.
(19) Deng, T. L. Phase equilibrium for the aqueous system containing lithium, sodium, potassium, chloride, and borate ions at 298 K. *J. Chem. Eng. Data* **2004**, *49*, 1295–1299.
(20) Lu, Z.; Luo, Y. F. Determination of taurine content by titration. *J. Math. Med.* **2000**, *4*, 350.
(21) Analytical Laboratory of Qinghai Institute of Salt Lakes at CAS. *The Analyses of Brines and Salts*, 2nd ed.; Science Press: Beijing, 1988; pp 35–41 and 64–66.
(22) Carton, A.; Sobron, F.; Bolado, S.; Tabars, J. Composition and density of saturated solutions of lithium sulfate + water + methanol. *J. Chem. Eng. Data* **1994**, *39*, 733–734.
(23) Hu, M. C.; Zhang, X. L.; Li, S. N.; Zhai, Q. G.; Jiang, Y. C.; Liu, Z. H. Solubility and refractive index for the ternary system propanol–rubidium nitrate–water at 25, 35, and 45 °C. *Russ. J. Inorg. Chem.* **2005**, *9*, 1434–1440.
(24) Ostroff, A. G.; Metler, A. V. Solubility of calcium sulfate dihydrate in the system NaCl–$MgCl_2$–H_2O from 28 to 70 °C. *J. Chem. Eng. Data* **1966**, *11*, 346–350.